

# Growth mechanisms of WC in WC–5.75 wt% Co

Yang Zhong, Leon L. Shaw\*

*Department of Chemical, Materials and Biomolecular Engineering University of Connecticut, Storrs, CT 06269, USA*

Received 11 April 2011; received in revised form 7 June 2011; accepted 9 June 2011

Available online 15 June 2011

## Abstract

The grain growth mechanisms of WC in WC–5.75 wt% Co are studied in this work. The two well known growth modes of WC in cemented carbides (coalescence process and solution/precipitation process) are both observed and show temperature dependence. At low temperatures (1100 and 1200 °C), the growth of WC grains is mainly through coalescence. At intermediate temperatures (1300 °C), coarsening of most WC grains takes place via isotropic growth, accompanied by the shape relaxation leading to the faceting of round grains. At high temperatures (1400 °C), layer-by-layer structures, resulting from anisotropic growth, are observed. Both isotropic growth at 1300 °C and anisotropic growth at 1400 °C are assisted by the solution/precipitation process. This is the first time that layer-by-layer structures are observed for WC crystals in WC–Co. The formation mechanism of layer-by-layer structures has been discussed based on the 2D nucleation and growth mechanism and the diffusion rates of W and C atoms within the Co binder at different temperatures.

© 2011 Elsevier Ltd and Techna Group S.r.l. All rights reserved.

**Keywords:** A. Grain growth; Tungsten carbide; Cermets; Crystal shape

## 1. Introduction

Tungsten carbide–cobalt (WC–Co) materials have been widely used in military, aerospace, automotive, marine, petrochemical, mining, electronics, and wood industries [1–4]. There is strong evidence showing that the size and shape of WC crystals within cemented carbides affects mechanical properties [5–12]. Hence, a better understanding of the growth behavior of WC crystals to enable the microstructure control is of great interest. Following by the pioneering work of Gurland et al. [13–15], the microstructure of WC in cemented carbides have been studied extensively in the last fifty years [16–29]. The equilibrium structure of WC has long been suggested to be truncated triangular prisms [7,14,16]. Recent density functional theory (DFT) studies [17,18], based on the surface energy minimization principles, show that the bulky truncated triangular prisms are indeed the equilibrium morphology of WC. These DFT studies further reveal that truncated triangular prisms can approach either near hexagonal or near triangular shapes, depending on the wetting conditions of the binder and the chemical potential of C [17,18]. However, the shape of WC

crystals in cemented carbides is not always the equilibrium shape, which is determined by a balance of shape relaxation (towards equilibrium structure) and carbide crystal growth process (towards growth-determined structure) [19]. Two modes are generally considered for the grain growth of WC in cemented carbides, namely, coalescence process and solution/precipitation process [20]. One school of thoughts considers that coalescence is the dominant mechanism [21], while others consider solution/precipitation is mostly responsible for the grain growth of WC [20,22].

The different viewpoints mentioned above indicate the necessity for further investigation. Towards this end, in this work we have systematically studied the growth mechanisms of WC in WC–5.75 wt% Co by investigating the microstructure evolution of WC crystals under different heating conditions (1100, 1200, 1300 and 1400 °C). This study covers the growth of WC crystals with Co in both solid and liquid states. Furthermore, this study investigates the growth behavior of WC crystals in a loose powder form. It is well known that densification and crystal growth happen simultaneously during liquid phase sintering of WC–Co. As a result, WC crystals are often in contact with each other during liquid phase sintering and the shape of WC grains can be truncated from the equilibrium form because of the presence of the neighboring WC grains. In order to avoid the complication of the shape

\* Corresponding author. Tel.: +1 860 486 2592; fax: +1 860 486 4745.

E-mail address: [leon.shaw@uconn.edu](mailto:leon.shaw@uconn.edu) (L.L. Shaw).

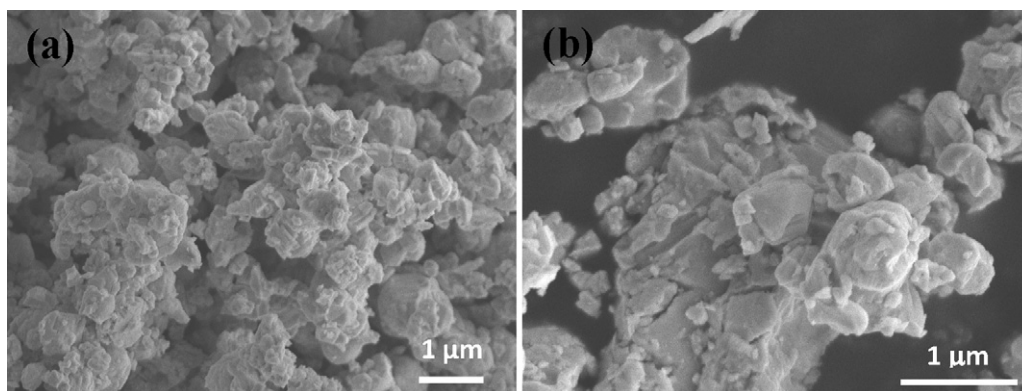


Fig. 1. SEM images of the as-received WC–Co powder.

alternation due to the truncating by other grains, the present study uses loose powder to investigate the growth behavior of WC crystals. Under this condition WC crystals on the top of the loose powder pile can grow with little or no geometric interference from the underneath WC grains. Therefore, this work can provide better insights into the growth behavior of WC crystals under different heating conditions. It is found that the growth mechanism of WC crystals in WC–Co depends strongly on temperature. Moreover, a new mechanism via layer-by-layer growth has been identified for the first time. This layer-by-layer growth phenomenon offers a direct evidence for the anisotropic growth of WC grains in WC–Co. The change of the growth mechanism as a function of temperature has been elucidated based on the thermodynamic driving force and the diffusion rates of W and C atoms mediated by the state of the Co phase.

## 2. Experimental

A commercial WC–5.75 wt% Co powder of 99.9% purity with the reported free carbon concentration of  $\sim 0.2$  wt% (Alfa Aesar, Ward Hill, MA) is used in experiments. Fig. 1(a and b) shows the SEM images of the as-received WC–Co powder. It can be seen that particle sizes range from 100 nm to 700 nm. The average particle size is estimated to be between 200 nm and 300 nm based on multiple SEM images. Most of the particles are round without clear facets. To study the microstructure evolution of WC particles as a function of temperature under carbon-deficient conditions, the powder is subjected to heat treatments at different temperatures (1100, 1200, 1300 and 1400 °C) for 2 h under an argon atmosphere in loose powder form. To create carbon-deficient conditions during grain growth, the powder was loaded in an  $\text{Al}_2\text{O}_3$  boat, then into an  $\text{Al}_2\text{O}_3$  tube furnace evacuated to  $10^{-3}$  Torr, and subsequently back filled with argon. The heating rate is  $10^\circ\text{C}/\text{min}$  for all the heat treatments. Under these operating conditions, a slight carbon-deficient condition is created (to be discussed more later). The morphology of the as-received and heat treated powders are characterized with the aid of a field-emission scanning electron microscope (FESEM, JEOL, JSM 6335F). Phase identification is carried out by employing X-ray diffraction (XRD) with Cu  $K\alpha$  radiation (Bruker Axs D5005D X-ray Diffractometer).

## 3. Results and discussion

### 3.1. Phase evolution

Fig. 2 shows the XRD patterns for the as-received WC–Co powder as well as the powder after the heat treatment at different temperatures. For the as-received WC–Co powder, only WC and Co peaks are found in the pattern. After heating, Co peaks disappear, which can be explained by the reaction of WC with Co to form ternary phases. A small amount of the  $\text{Co}_6\text{W}_6\text{C}$  ( $\text{M}_{12}\text{C}$ ) phase is found at low temperatures (1100 and 1200 °C), while small amounts of  $\text{Co}_2\text{W}_4\text{C}$  and  $\text{Co}_3\text{W}_3\text{C}$  ( $\text{M}_6\text{C}$ ) phases are found at 1300 and 1400 °C, respectively. The formation of these small amounts of ternary carbides ( $\eta$  phase) is due to the decarburization of the WC powder during the heat treatment because our previous study [23] reveals that the sequence of WC formation through the carburization of W and  $\text{Co}_3\text{W}$  is  $\text{W} + \text{Co}_3\text{W} \rightarrow \text{Co}_6\text{W}_6\text{C}(\text{M}_{12}\text{C}) \rightarrow \text{Co}_3\text{W}_3\text{C}(\text{M}_6\text{C}) \rightarrow \text{W}_2\text{C} + \text{Co} \rightarrow \text{WC} + \text{Co}$ . Thus, it is reasonable to expect that the decarburization will result in the formation of  $\text{M}_6\text{C}$  and  $\text{M}_{12}\text{C}$ . Based on these observations, it can be concluded that the growth of WC grains in this study is under carbon-deficient conditions. Note that the effect of carbon concentration on the

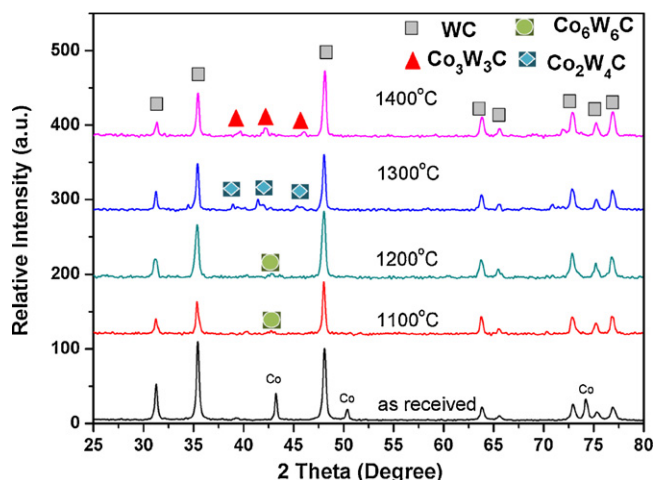


Fig. 2. XRD patterns of the WC–Co loose powder in the as-received form and after heating at different temperatures (1100, 1200, 1300 and 1400 °C) for 2 h.

growth of WC crystals has been addressed by several different studies [24–27]. Thus, this study will only focus on the WC growth under carbon-deficient conditions.

### 3.2. Temperature dependence of growth mechanisms

The as-received WC–Co powder is rounded without clear facets, as shown in Fig. 1. Fig. 3(a and b) shows the SEM images of WC–Co powder after heating at 1100 and 1200 °C for 2 h, respectively. Note that some WC particles have changed from the round morphology to the multi-faceted morphology. The close examination reveals that these multi-faceted particles frequently exhibit highly irregular shapes with one side having multiple steps and the other side having a flat surface (shown in Fig. 3(b)). It is clear that these shapes deviate from the equilibrium shape (truncated triangular prisms) and are considered to be the products of coalescence of small particles. The present observation of coalescence is consistent with the previous reports [7,28,29], showing that coalescence of small WC particles can take place during the early stage heating of fine WC–Co powder particles.

Two important factors are responsible for coalescence at low temperatures. (i) Coalescence does not require long distance diffusion of atoms, and therefore can be potentially achieved at low temperatures. (ii) The kinetic barrier for coalescence is from the slight shifting and/or rotating of neighboring particles and requires either low misorientation angles or small neighboring particles for easy rotation. This factor requires that neighboring particles have to be small for rotation to take place. This is why coalescence has been frequently observed for nano-materials [30,31] and fine WC–Co particles [7,28]. During the coalescence, the small particles merge into one larger particle by aligning their orientations through slight shifting and/or rotating. The shape of the newly formed larger particle often inherits the geometrical features of smaller particles. As such, highly irregular and unsymmetrical particles are formed. Coalescence is energetically favored because the formation of larger crystals will reduce the surface energy of the system. Finally, it should be pointed out that due to the low cobalt content in our powder, carbide to carbide grain boundaries are more prevalent compared with higher cobalt content powders. Thus, the low cobalt content may have

contributed to the extensive coalescence of fine WC crystals observed in this study.

Fig. 4 presents the SEM images of the WC–Co powder after heating at 1300 °C for 2 h. It is noted that most of the characteristics of coalescence observed at 1100 and 1200 °C have disappeared. Many WC grains at 1300 °C (~70%) exhibit the coarsened and round morphology (labeled with circles), while some WC grains show close to the equilibrium structure (i.e., truncated triangular prisms, ~25%, labeled with triangles) or the layer-by-layer structure (<5%, labeled with rectangles). The last morphology is clearly the product of anisotropic growth, whereas the round morphology is the product of isotropic growth. Since most of WC grains appear with round morphology, it can be concluded that the dominant coarsening mechanism for WC grains at 1300 °C is isotropic growth.

It should be pointed out that the mechanism for the formation of truncated triangular prisms is less clear than that of the layer-by-layer structure and the round morphology. Given the fact that the equilibrium shape of WC is a truncated triangular prism rather than round morphology [17,18], truncated triangular prisms can result from faceting of round WC grains driven by the surface energy minimization. However, we cannot rule out the possibility of truncated triangular prisms resulting directly from the anisotropic crystal growth process. In any case, faceting is not observed at 1100 and 1200 °C, but becomes possible at 1300 °C. This is attributed to the increased mobility of atoms for diffusion at 1300 °C. This increased mobility can be ascribed to the presence of thin solid Co films which can allow solid-state solution/precipitation to take place at 1300 °C, slightly below the eutectic point of WC–Co, ~1330 °C [32,33]. Without the presence of Co, WC grains exhibit litter growth at 1300 °C [28], indicating the importance of Co even at the solid-state. Our data suggests that the reprecipitation of WC from the Co–W–C solid solution at 1300 °C occurs on the surfaces of both round and faceted crystals, leading to crystals with both smooth and faceted morphologies.

Fig. 5(a and b) shows the SEM images of the WC–Co powder after heating at 1400 °C for 2 h. Layer-by-layer structures (arrows indicated in Fig. 5(a)) have increased drastically over those seen at 1300 °C. The existence of the layer-by-layer structure unambiguously reveals the anisotropic

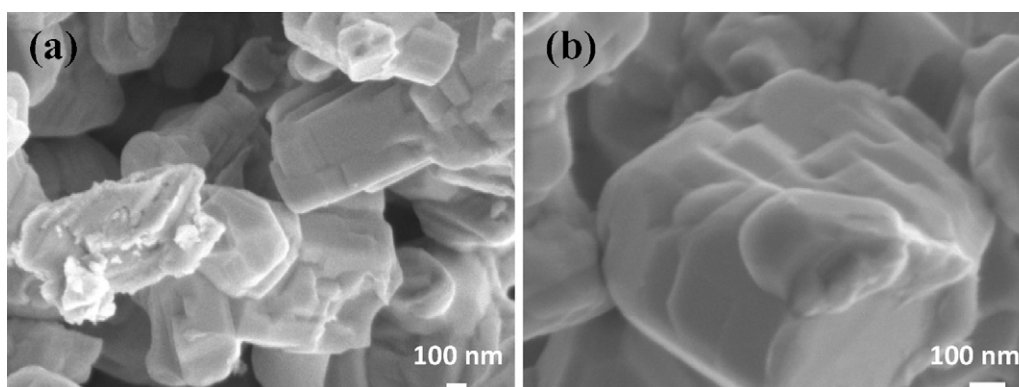


Fig. 3. SEM images of the as-received WC–Co powder: (a) after heating at 1100 °C for 2 h, and (b) after heating at 1200 °C for 2 h.



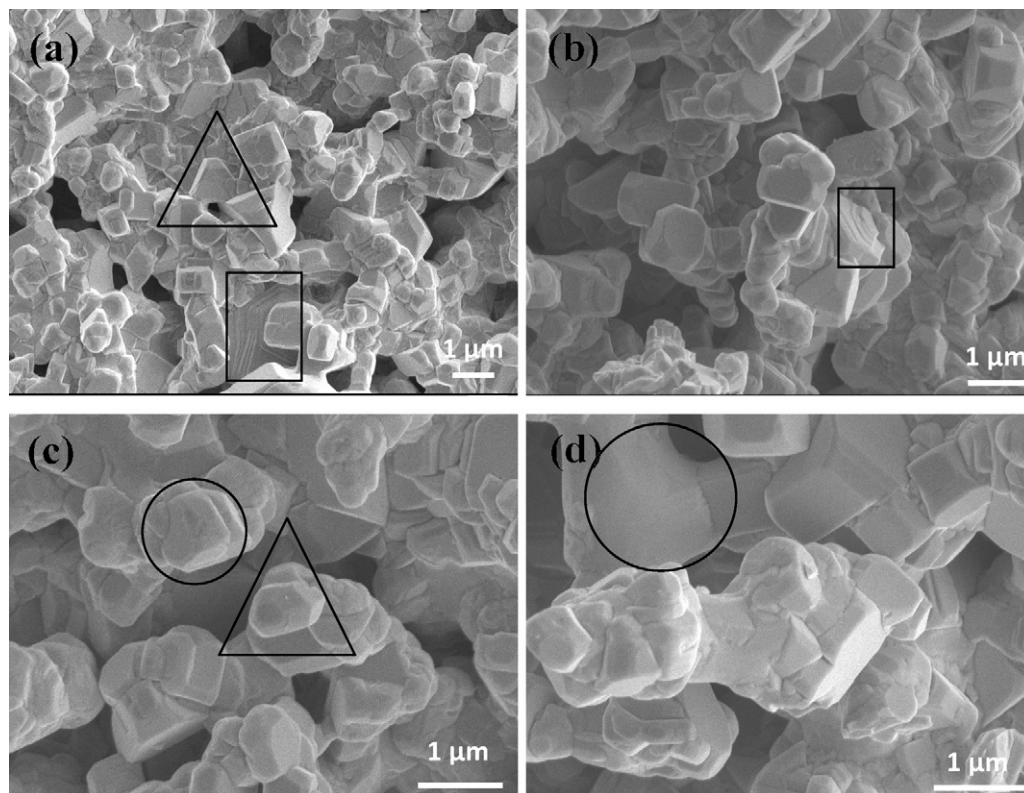


Fig. 4. SEM images of the WC–Co powder after heating at 1300 °C for 2 h. Multiple images are shown in order to highlight the presence of WC crystals with different morphologies.

growth of WC grains at 1400 °C. It is well established that WC has a HCP crystal structure with two sets of three equivalent  $(10\bar{1}0)$  planes rather than six equivalent  $(10\bar{1}0)$  planes [7,14,16]. Because of this unique nature of the crystal structure, WC crystals grown from liquid metal solutions and WC grains in WC–Co often have the equilibrium shape of truncated triangular prisms with  $(0001)$  planes as their bases [18,19]. Since all of the layered structures in Fig. 5(a and b) have near hexagonal morphologies, it is reasonable to argue that the  $(0001)$  plane stacking in the  $\langle 0001 \rangle$  direction is the growth direction for the layer-by-layer structure. It is noted that there are many tiny particles ( $<100$  nm) on the surface of large WC

particles at the 1400 °C heated samples (Fig. 5(a and b)). EDS analysis reveals that these tiny particles are the Co-rich phase. Thus, these tiny particles are likely the precipitates during cooling from the liquid Co films on the surface of WC particles at 1400 °C.

The existence of the layer-by-layer structure suggests that the anisotropic growth of WC proceeds via the 2D nucleation and growth mechanism. It is well known that a large thermodynamic driving force is required for the 2D nucleation and growth mechanism to happen [34]. Such a large driving force can be postulated to come from the following processes. During the heating stage (lasting for 140 min before reaching

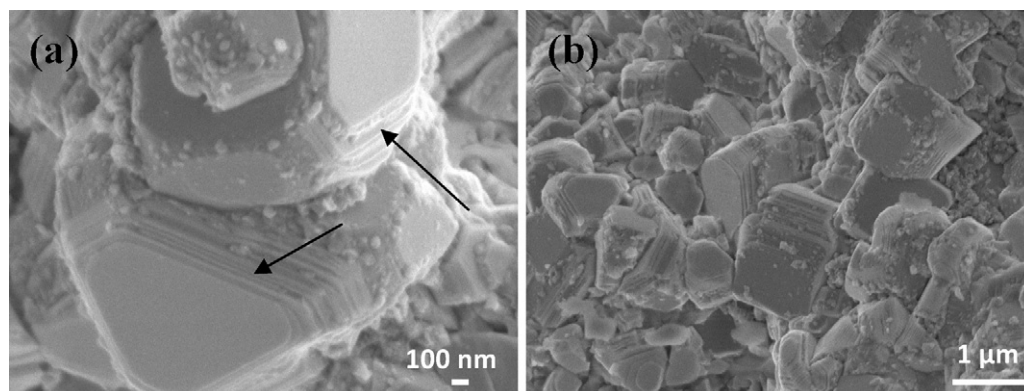


Fig. 5. SEM images of the as-received WC–Co powder after heating at 1400 °C for 2 h. Two magnifications are present in order to provide (a) a close look at and (b) general view of the characteristics of the powder.

1400 °C) WC particles coarsen via coalescence and then via isotropic growth enhanced by solution/precipitation while simultaneously changing from round crystals to faceted ones. This allows some WC crystals to grow larger while some become smaller, creating a large surface energy difference between large and small crystals and thus laying the foundation for the 2D nucleation and growth mechanism to take off at 1400 °C. This proposed pathway is consistent with the observed change of the crystal growth mechanism as a function of temperature in this study, and in good accordance with the report by Park et al. [35] who show that the abnormal growth of WC crystals via the 2D nucleation and growth mechanism can be enhanced by the direct use of powder with a bimodal grain size distribution or by holding fine WC particle samples (1.3  $\mu\text{m}$ ) at 1450 °C for 10 h to allow crystal growth and to create a mixture of large and small crystals in the powder.

### 3.3. Layer-by-layer growth

Although the layer-by-layer structure is observed for the first time for WC crystals, such structures are frequently found in the epitaxial growth of metals and are considered as the products of 2D nucleation with either 2D or 3D growth [36–38]. In this study, detailed examination of the layer-by-layer structures suggests that the growth mechanism of the layer-by-layer structure is temperature dependent, i.e., the layer-by-layer structures at 1300 °C are produced from 2D nucleation with 3D growth, whereas those at 1400 °C are generated from 2D nucleation with 2D growth. This viewpoint is elaborated below in detail.

First, the layer-by-layer structures formed at 1300 °C are different from those at 1400 °C. At 1300 °C a new island is formed on top of another island, and the size of the central top island is much smaller than the size of the base of the truncated triangular prism. This suggests that the growth of the crystal happens in two directions simultaneously, that is, existing islands spread out in their respective layers while a new island is nucleated at the center of the top layer. However, this is not the case at 1400 °C where it appears that each layer grows very fast once it is nucleated. Since at 1300 °C a new layer nucleates well before the growth of preceding ones is completed, the growth is considered to be three-dimensional (3D). In contrast, the growth at 1400 °C is two-dimensional (2D) because a new layer will not nucleate until the growth of the preceding layer is largely completed. Kunkel et al. [36] propose that the decisive factor for 2D or 3D growth of the layer-by-layer structure is the thermal energy of the adatoms. If the thermal energy is large enough to overcome the barrier to jump to the layer below, there is no nucleation until the growth completion of the preceding layer. This condition results in 2D growth; otherwise, 3D growth takes place. This proposed mechanism is consistent with our observations, that is, higher thermal energies of W and C atoms at 1400 °C lead to 2D growth and lower thermal energies at 1300 °C result in 3D growth.

Second, for the layer-by-layer growth (both 2D and 3D) of the WC crystals on the top of the loose powder pile as observed in this study, W and C atoms need to diffuse from small WC

crystals to the (0 0 0 1) surfaces of large faceted crystals via their (1 0  $\bar{1}$  0) surfaces. This diffusion path creates WC concentration gradients from the edges to the center of the (0 0 0 1) surface. Furthermore, at 1300 °C diffusion proceeds through solid-state Co thin films on the surface of WC crystals, while at 1400 °C diffusion is through liquid Co thin films. When W and C atoms diffuse from different edges towards the center, it is relatively easy for a large number of the dissolved atoms to reach the saturation point at the center and form the nucleus with the critical radius for nucleation. Hence, the layer-by-layer growth starts at the center of the layer, which has been seen in Fig. 4. After nucleation at the center of the (0 0 0 1) surface, the island will grow across the layer until they reach the edges. The growth process is expected to be affected by temperature. At 1400 °C the presence of liquid Co thin films can provide fast diffusion paths for W and C, and thus offer ample supplies of W and C for rapid growth of each layer. As a result, one observes dominant 2D growth at 1400 °C. In contrast, at 1300 °C the diffusion rate is much slower because diffusion is via solid-state Co thin films and at lower temperatures. Under this condition, nucleation takes place at the same fashion as at 1400 °C since no crystal defects, such as screw dislocations, edge dislocations and twin boundaries, are observed to form surface edges to promote the 3D growth [39–44]. The growth of the island, however, is very slow because of the lower diffusion rate and thus limited supplies of W and C atoms. As such, a new island nucleates well before the growth of preceding ones is completed, and thus 3D growth is observed at 1300 °C.

### 4. Concluding remarks

The growth behavior of WC crystals in WC–5.75 wt% Co under carbon-deficient conditions has been studied systematically. The growth mechanism is found to change with temperature. The evolution of the growth mechanism as a function of temperature can be summarized in Fig. 6. At lower temperatures (1100 and 1200 °C), WC forms irregular morphology via coalescence of small crystals. At intermediate

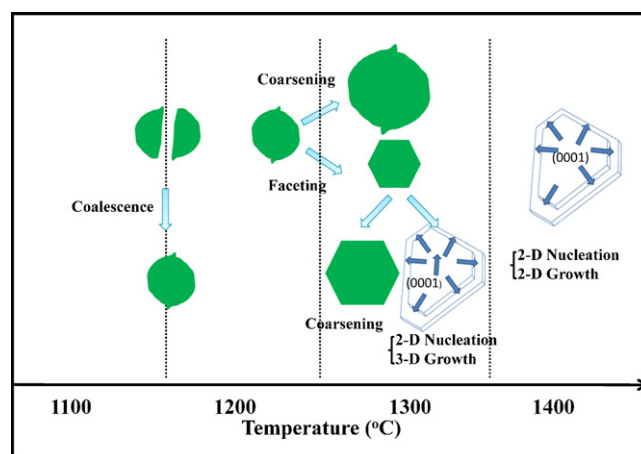


Fig. 6. Schematic drawing of the growth mechanisms of WC in WC–Co under different heating conditions.

temperatures (1300 °C), coarsening of most WC crystals takes place via isotropic growth, leading to the formation of large round crystals. At the same time, the shape relaxation occurs, resulting in the faceting of round grains. In addition, a very small number of WC crystals exhibit the layer-by-layer structure, indicating that anisotropic growth can start at 1300 °C. At high temperatures (1400 °C) the layer-by-layer structure becomes dominant. The layer-by-layer structure at 1300 °C is found to form by 2D nucleation with 3D growth, whereas the layer-by-layer structure at 1400 °C is created by 2D nucleation with 2D growth. The different growth mechanism can be explained by the different diffusion rates of W and C atoms in the solid-state Co thin films at 1300 °C and in the liquid Co thin films at 1400 °C. The layer-by-layer structure is not the equilibrium structure, but the growth-controlled morphology. It takes place at high temperatures because it requires high thermodynamic driving forces. Both isotropic and anisotropic growth at intermediate and high temperatures are assisted with the solution/precipitation mechanism. This study indicates that the coarsening mechanism of WC crystals is temperature dependent with the presence of both coalescence and solution/precipitation in one WC–Co material. Furthermore, the state of the binder phase (Co) can strongly affect the growth behavior of WC crystals in the WC–Co system.

## Acknowledgements

This research was sponsored by the U.S. National Science Foundation (NSF) under the contract number CMMI-0856122. The support and vision of Dr. Mary Toney is greatly appreciated.

## References

- [1] P. Schwarzkopf, R. Kieffer, *Refractory Hard Metals*, Macmillan, New York, 1953.
- [2] D.H. Jack, Cemented carbide as an engineering material, in: M.M. Schwartz (Ed.), *Engineering Applications of Ceramic Materials: Source Book*, American Society for Metals, Materials Park, OH, 1985 pp. 147–153.
- [3] *Metals Handbook, Properties and Selection: Stainless Steels, Tool Materials and Special-Purpose Metals*, vol. 3, 9th ed., American Society for Metals, Materials Park, OH, 1980.
- [4] S.W.H. Yih, C.T. Wang, *Tungsten Sources, Metallurgy, Properties and Applications*, Plenum Press, New York, 1979.
- [5] Z.Z. Fang, X. Wang, R. Ryu, K.S. Hwang, H.Y. Sohn, Synthesis, sintering, and mechanical properties of nanocrystalline cemented tungsten carbide—A review, *Int. J. Refract. Met. Hard Mater.* 27 (2009) 288–299.
- [6] J. Weidow, S. Norgren, H.O. Andren, Effect of V, Cr and Mn additions on the microstructure of WC–Co, *Int. J. Refract. Met. Hard Mater.* 27 (2009) 817–822.
- [7] H.E. Exner, Physical and chemical nature of cemented carbides, *Int. Met. Rev.* 24 (1979) 149–173.
- [8] S. Kinoshita, T. Saito, M. Kobayashi, K. Hayashi, Microstructure and mechanical properties of new WC–Co base cemented carbide having highly oriented plate-like triangular prismatic WC grains, *J. Jpn. Soc. Powder Powder Metall.* 47 (2000) 526–533.
- [9] K. Kitamura, M. Kobayashi, K. Hayashi, Microstructural development and properties of new WC–Co base hardmetal prepared from  $\text{Co}_x\text{W}_y\text{C}_z + \text{C}$  instead of WC, *J. Jpn. Soc. Powder Powder Metall.* 48 (2001) 621–628.
- [10] F.A. da Costa, F.F.P. de Medeiros, A.G.P. da Silva, U.U. Gomes, M. Filgueira, C.P. de Souza, Structure and hardness of a hard metal alloy prepared with a WC powder synthesized at low temperature, *Mater. Sci. Eng. A* 485 (2008) 638–642.
- [11] B. Reichel, K. Wagner, D.S. Janisch, W. Lengauer, Alloyed W–(Co, Ni, Fe)–C phases for reaction sintering of hardmetals, *Int. J. Refract. Met. Hard Mater.* 28 (2010) 638–645.
- [12] V. Bonache, M.D. Salvador, D. Busquets, P. Burguete, E. Martinez, F. Sapina, E. Sanchez, Synthesis and processing of nanocrystalline tungsten carbide: towards cemented carbides with optimal mechanical properties, *Int. J. Refract. Met. Hard Mater.* 29 (2011) 78–84.
- [13] J. Gurland, P. Bardzil, Relation of strength, composition, and grain size of sintered WC–Co alloys, *Trans. AIME* 203 (1955) 311–315.
- [14] J. Gurland, Comparison of the strength of sintered carbides, *Trans. AIME* 209 (1957) 512–513.
- [15] J. Gurland, The fracture strength of sintered tungsten carbide–cobalt alloys in relation to composition and particle spacing, *Trans. AIME* 227 (1963) 1146–1150.
- [16] H.E. Exner, Struktur und eigenschaften der hartlegierung WC–10%Co, *Jernkontoret Technical Report JK U8* (1964) 64–20.
- [17] M. Christensen, G. Wahnstrom, C. Allibert, S. Lay, Quantitative analysis of WC grain shape in sintered WC–Co cemented carbides, *Phys. Rev. Lett.* 94 (2005) 066105.
- [18] Y. Zhong, H. Zhu, L.L. Shaw, R. Ramprasad, The equilibrium morphology of WC particles—a combined *ab initio* and experimental study, *Acta Mater.* 59 (2011) 3748–3757.
- [19] A.V. Shatov, S.A. Firstov, I.V. Shatova, The shape of WC crystals in cemented carbides, *Mater. Sci. Eng. A* 242 (1998) 7–14.
- [20] R. Warren, M.B. Waldron, Microstructural development during the liquid-phase sintering of cemented carbides, *Powder Metall.* 15 (1972) 166–201.
- [21] M. Humenik, N.M. Parikh, *Cermets: I, fundamental concepts related to micro-structure and physical properties of cermet systems*, *J. Am. Ceram. Soc.* 39 (1956) 60–63.
- [22] H.E. Exner, H.F. Fischmeister, The mechanical properties of cemented tungsten carbide–cobalt alloys in relation to the structure, *Arch. Eisenhüttenwes* 37 (1966) 499–506.
- [23] Z.G. Ban, L.L. Shaw, On the reaction sequence of WC–Co formation using an integrated mechanical and thermal activation process, *Acta Mater.* 49 (2001) 2933–2939.
- [24] Y. Wang, M. Heusch, S. Lay, C.H. Allibert, Microstructure evolution in the cemented carbides WC–Co I. Effect of the C/W ratio on the morphology and defects of the WC grains, *Phys. Status Solidi (a)* 2 (2002) 271–283.
- [25] G.J. Rees, B. Young, Study of the factors controlling grain size in sintered hard-metal, *Powder Metall.* 14 (1971) 185–198.
- [26] E. Lardner, Control of grain size in the manufacture of sintered hard metal, *Powder Metall.* 13 (1970) 394–428.
- [27] J. Lee, D. Jaffery, J.D. Browne, Influence of process variables on sintering of WC–25 wt% Co, *Powder Metall.* 23 (1980) 57–64.
- [28] X. Wang, Z.Z. Fang, H.Y. Sohn, Grain growth during the early stage of sintering of nanosized WC–Co powder, *Int. J. Refract. Met. Hard Mater.* 26 (2008) 232–241.
- [29] W.D. Shubert, A. Bock, B. Lux, General aspects and limits of conventional ultrafine WC powder manufacture and hard metal production, *Int. J. Refract. Met. Hard Mater.* 13 (1995) 281–296.
- [30] Z. Zhang, H. Sun, X. Shao, D. Li, H. Yu, M. Han, Three-dimensionally oriented aggregation of a few hundred nanoparticles into monocrystalline architectures, *Adv. Mater.* 17 (2005) 42–47.
- [31] Y. Cheng, Y. Wang, Y. Zheng, Y. Qin, Two-step self assembly of nanodisks into plate-built cylinders through oriented aggregation, *J. Phys. Chem. B* 109 (2005) 11548–11551.
- [32] R.F. Snowball, D.R. Milner, Densification processes in the tungsten carbide–cobalt system, *Powder Metall.* 11 (1968) 23–40.
- [33] L. Froschauer, R.M. Fulrath, Direct observation of liquid-phase sintering in the system tungsten carbide–cobalt, *J. Mater. Sci.* 11 (1976) 142–149.
- [34] D.A. Porter, K.E. Easterling, *Phase Transformations in Metals and Alloys*, Chapman and Hall, London, 1990.

- [35] Y.J. Park, N.M. Hwang, D.Y. Yoon, Abnormal growth of faceted (WC) grains in a (Co) liquid matrix, *Metall. Mater. Trans. A* 27 (1996) 2809–2819.
- [36] R. Kunkel, B. Poelsema, L.K. Verheij, G. Comsa, Reentrant layer-by-layer growth during molecular-beam epitaxy of metal-on-metal substrates, *Phys. Rev. Lett.* 65 (1990) 733–736.
- [37] J. Tersoff, A.W. Denier van Gon, R.M. Tromp, Critical island size for layer-by-layer growth, *Phys. Rev. Lett.* 72 (1994) 266–269.
- [38] H.A. van der Vegt, H.M. van pinxteren, M. Lohmeier, E. Vlieg, Surfactant-induced layer-by-layer growth of Ag on Ag(1 1 1), *Phys. Rev. Lett.* 68 (1992) 3335–3338.
- [39] F.C. Frank, The influence of dislocations on crystal growth, *Discuss. Faraday Soc.* 5 (1949) 48–54.
- [40] W.K. Burton, N. Cabrera, F.C. Frank, The growth of crystals and the equilibrium structure of their surfaces, *Philos. Trans. R. Soc. London A* 243 (1951) 299–358.
- [41] E. Bauser, H. Strunk, Dislocations as growth step sources in solution growth and their influence on interface structures, *Thin Solid Films* 93 (1982) 185–294.
- [42] F.C. Frank, Edge dislocations as crystal growth sources, *J. Cryst. Growth* 51 (1981) 367–368.
- [43] R.S. Wager, On the growth of germanium dendrites, *Acta Metall.* 8 (1960) 57–60.
- [44] D.R. Hamilton, R.G. Seidensticker, Propagation mechanism of germanium dendrites, *J. Appl. Phys.* 31 (1960) 1165–1168.